

Subcutaneous Tissue Mechanical Behavior is Linear and Viscoelastic Under Uniaxial Tension

James C. Iatridis,¹ Junru Wu,² Jason A. Yandow,³ and Helene M. Langevin³

Department of Mechanical Engineering,¹ Physics,² and Neurology,³ University of Vermont, Burlington, Vermont, USA

Subcutaneous tissue is part of a bodywide network of “loose” connective tissue including interstitial connective tissues separating muscles and surrounding all nerves and blood vessels. Despite its ubiquitous presence in the body and its potential importance in a variety of therapies utilizing mechanical stretch, as well as normal movement and exercise, very little is known about loose connective tissue’s biomechanical behavior. This study aimed to determine elastic and viscoelastic mechanical properties of ex-vivo rat subcutaneous tissue in uniaxial tension with incremental stress relaxation experiments. The elastic response of the tissue was linear, with instantaneous and equilibrium tensile moduli of 4.77 kPa and 2.75 kPa, respectively. Using a 5 parameter Maxwell solid model, material parameters $\mu_1 = 0.95 \pm 0.24$ Ns/m and $\mu_2 = 8.49 \pm 2.42$ Ns/m defined coefficients of viscosity related to time constants $\tau_{1M} = 3.83 \pm 0.15$ sec and $\tau_{2M} = 30.15 \pm 3.16$ sec, respectively. Using a continuous relaxation function, parameters $C = 0.25 \pm 0.12$, $\tau_{1C} = 1.86 \pm 0.34$ sec, and $\tau_{2C} = 110.40 \pm 25.59$ sec defined the magnitude and frequency limits of the relaxation spectrum. This study provides baseline information for the stress-strain behaviors of subcutaneous connective tissue. Our results underscore the differences in mechanical behaviors between loose and high-load bearing connective tissues and suggest that loose connective tissues may function to transmit mechanical signals to and from the abundant fibroblasts, immune, vascular, and neural cells present within these tissues.

Keywords Fascia, Skin, Subcutaneous Connective Tissue, Tensile Material Properties, Viscoelastic.

INTRODUCTION

Although tensile properties of specialized connective tissue (bone, cartilage, tendon, vertebral disc) have been extensively studied, very little is known about the biomechanical behavior of

“loose” connective tissue. Loose connective tissue forms a continuous bodywide network including subcutaneous and interstitial connective tissues surrounding all muscles, organs, nerves, blood vessels, and lymphatics [6]. This connective tissue network is remarkable in that it is highly cellular (with abundant fibroblasts, adipocytes, and immune cells) and at the same time constitutes the collagenous matrix through which immune, endocrine, and paracrine signaling molecular exchange take place. Mechanical forces are increasingly recognized as important regulators of intracellular processes including signaling pathway activation and gene expression [2]. The transduction of mechanical signals within loose connective tissue therefore is likely to have important and widespread effects on connective tissue cells as well as on vascular and neural elements present within this connective tissue.

Loose subcutaneous and intermuscular connective tissues undergo stretching under physiological conditions during breathing, body movements, and exercise. Therapeutic stretching of these connective tissues also is thought to occur in some physiotherapy techniques [12, 28], as well as in many “alternative” therapies such as massage, myofascial release, Rolfing, and yoga [21]. Acupuncture needling also has been shown to result in measurable winding and deformation of loose connective tissue [18]. It is unknown whether these various techniques act by applying suprphysiological amounts of stretch to tissues or by providing physiological amounts of stretch to tissues that are “stress-deprived” (as in therapeutic immobilization, reflex immobilization due to pain, or sedentary lifestyle). Understanding the biomechanical behavior of loose connective tissue is an important first step toward understanding the biomechanical, cellular, and molecular effects of therapies utilizing mechanical stretching, as well as of normal movements and exercise.

The objectives of our study were to determine elastic and viscoelastic mechanical properties of ex-vivo rat subcutaneous tissue in uniaxial tension. A rat subcutaneous tissue model was chosen because it allows future in vivo and in vitro studies investigating the biological response to mechanical loading on this

Received 17 December 2002; revised 24 June 2003; accepted 3 July 2003.

Address correspondence to James C. Iatridis, Assistant Professor, Dept. of Mechanical Engineering, 231B Votey Building, 33 Colchester Ave., University of Vermont, Burlington, VT 05405-0156, USA. E-mail: james.iatridis@uvm.edu

tissue. The abdomen was chosen because its large surface allowed uniform and repeatable dissection in several regions. Uniaxial tension was chosen as the loading mode because stretching of this collagenous network, e.g., as with treatments such as massage or acupuncture, is anticipated *in vivo*. The first goal was to assess the equilibrium and instantaneous elastic response of this tissue and the second goal was to define its viscoelastic behavior.

METHODS

Specimen Preparation

Subcutaneous connective tissue was harvested from the abdomen of each of 5 male rats ranging in weight from 200–250 g immediately after death. Four specimens were harvested from ventral and lateral regions on the left and right sides of each animal to obtain 20 total specimens (Figure 1). First, a flap containing dermis, subcutaneous muscle, and subcutaneous tissue was dissected away from the abdominal wall musculature. Subcutaneous tissue then was dissected away from the subcutaneous muscle, while applying minimal traction on the tissue. Specimens were equilibrated in HEPES buffer pH7.4 at 20°C to promote cell viability and establish dimensional stability. This dissection technique provided a sheet of subcutaneous tissue of nearly uniform thickness from which test specimens were harvested. Once the subcutaneous tissue was isolated, specimens were cut into rectangular strip-shaped specimens. Original width dimensions of the specimens were taken using a micrometer.

Mean \pm SD tissue width was 10.2 ± 0.9 mm for all specimens. Initial tissue length (length between grips) was prescribed at 20 mm. Initial cross-sectional area (for stress calculations) was determined by immersed volume of the unloaded specimen (after mechanical testing) divided by the initial tissue length (assuming the volume was constant after equilibration in HEPES buffer). The specimen volume was determined using the Archimedes principle. Only the volume of the gauge section (i.e., specimen cut at the grips) was measured. Volume measurements were made after mechanical testing because it was necessary to have extra tissue length for gripping the specimen during testing. Tissue thickness was determined by dividing the cross-sectional area by the mean specimen width, and it was 0.95 ± 0.68 mm for all specimens. Ventral and lateral regions were chosen because they provided the most uniform thickness of the tissue. Dorsal regions of the torso were avoided, as subcutaneous tissue in this region was both thinner and more variable in thickness.

Material Testing

Specimens were loaded into a set of custom tensile grips on a material testing machine (MTS, Eden Prairie, MN, USA). Tensile grips were designed to be similar to that described by Roth and Mow [23]; however, in our configuration, the grips held the specimen in place using constant displacement (rather than constant force) and also used a layer of Neoprene rubber to increase the frictional force between the grips and specimen to prevent slippage (Figure 2). Preliminary tests demonstrated that

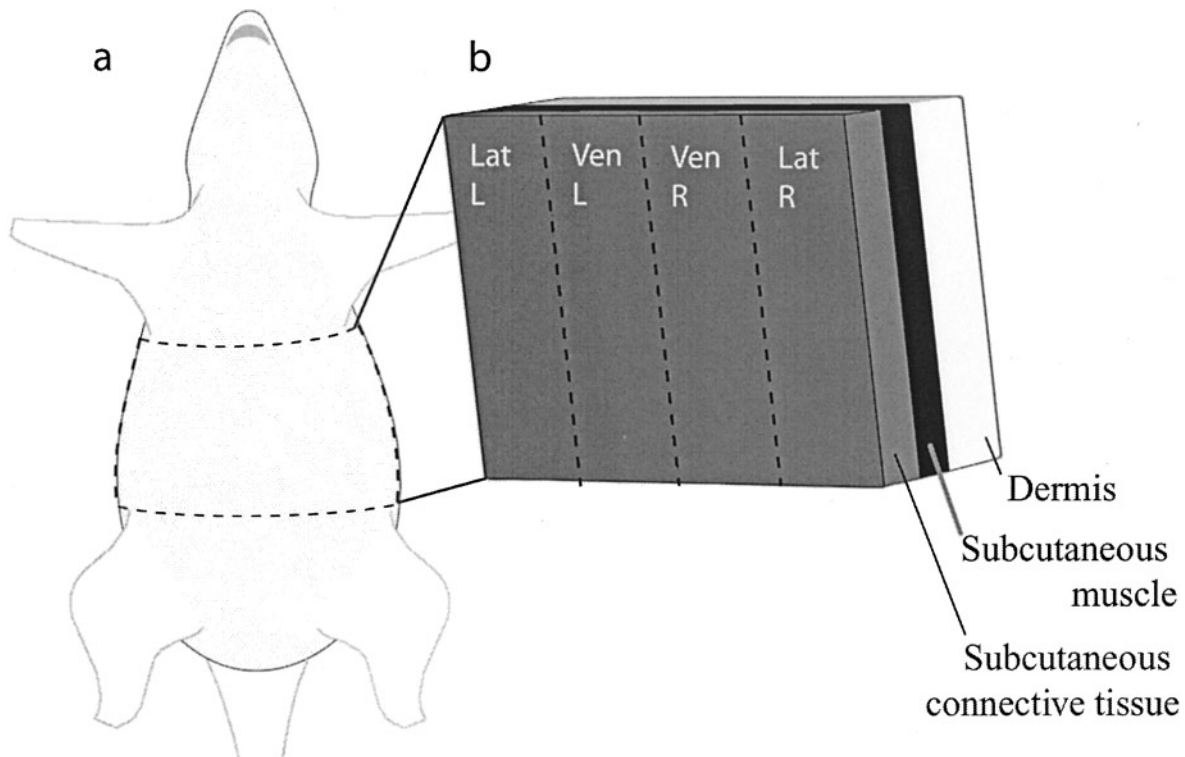


Figure 1. Schematic diagram describes (a) location of harvest of subcutaneous tissue and (b) layers of subcutaneous tissue comprising our test specimens.

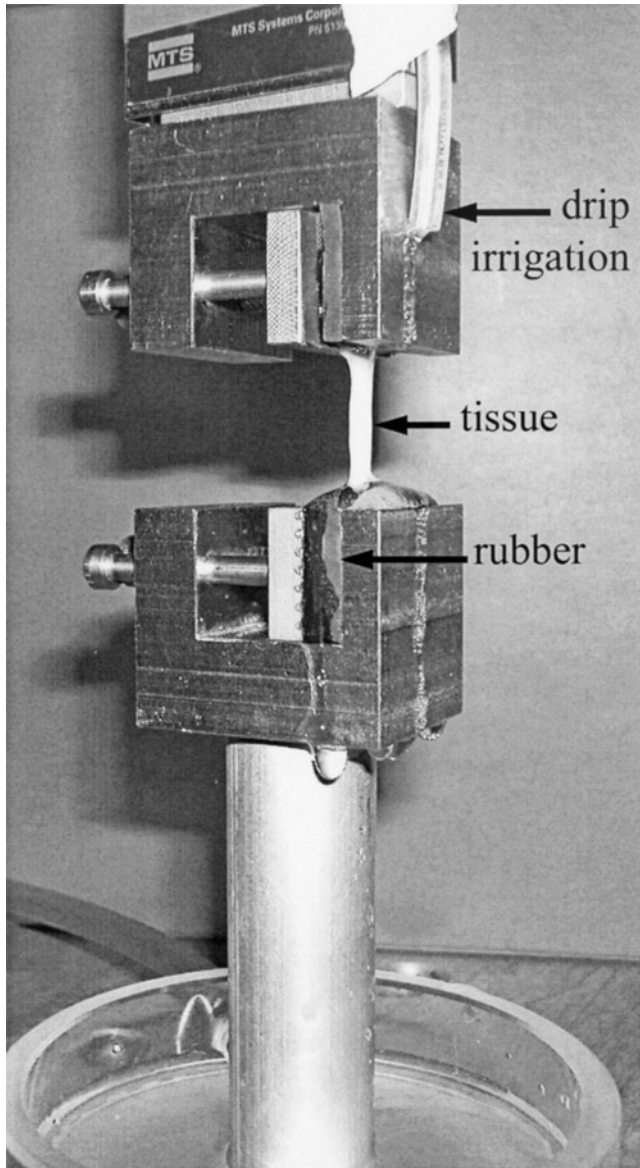


Figure 2. Photograph of sample being loaded in the custom tensile grips on the material testing system. The grips held the specimen in place using a layer of neoprene rubber to increase the frictional force between the grips and specimen to prevent slippage. Specimens were loaded into the test frame at a prescribed length of 20 mm and irrigated with HEPES buffer throughout testing.

no slippage occurred during our tensile testing protocol. Specimens were loaded into the test frame at a prescribed length of 20 mm and irrigated with HEPES buffer throughout testing. Specimens were subjected to a preload of 0.044 N and to preconditioning of 10 cycles of 2 mm oscillatory displacement at a frequency of 1 Hz, followed by a 60-sec wait. Each tissue sample was then subjected to one test consisting of 10 incremental stress-relaxation steps. During each step the tissue was stretched by a 1 mm displacement increment followed by a 60-sec hold period of constant displacement (Figure 3). The 1 mm displace-

ments increments occurred in 1 sec and approached a “step” displacement input.

Constitutive Models

The linearity of the instantaneous and equilibrium elastic stress-strain relationships justified use of a linear viscoelastic constitutive model. The instantaneous tensile modulus, E^e , was determined by fitting a line to the experimental instantaneous stress-strain response. The reduced relaxation function was fit with two different viscoelastic models—a 5 parameter Maxwell solid model and a continuous relaxation function. Linear viscoelastic models based on Boltzmann’s superposition principle have been cited extensively in the literature to describe the mechanical behavior of many biological tissues. In this study, the tensile stress of subcutaneous connective tissue was modeled with an integral formulation of a linear viscoelastic constitutive model.

$$\sigma(t) = \int_{-\infty}^t G(t - \tau) E^e \frac{\partial \varepsilon(\tau)}{\partial \tau} d\tau \quad (1)$$

where $\sigma(t)$ is the tensile stress, $\varepsilon(t)$ is the tensile strain, E^e is the instantaneous elastic tensile modulus, and $G(t)$ is the reduced relaxation function. In this linear formulation, a step strain yields an instantaneous stress response proportional to the magnitude of applied strain, where E^e is the proportionality constant.

Reduced Relaxation Function for 5 Parameter Maxwell Solid Model

The generalized Maxwell model is one of the most useful models for describing viscoelastic behaviors and assumes a distribution (or discrete spectrum) of relaxation times instead of a single value [3, 10]. Based on this generalized model, we chose a discrete reduced relaxation function given by a 5 parameter Maxwell solid model (Figure 4) because fewer parameters did not adequately describe our material behavior and more parameters did not improve the ability of the model to describe the material behavior:

$$G(t) = \frac{G_0 + (\mu_1/\tau_{1M})e^{-t/\tau_{1M}} + (\mu_2/\tau_{2M})e^{-t/\tau_{2M}}}{G_0 + (\mu_1/\tau_{1M}) + (\mu_2/\tau_{2M})} \quad (2)$$

where G_0 is a fitting parameter related to the equilibrium normalized elasticity constant, and parameters μ_1 and μ_2 define the coefficients of viscosity related to time constants τ_{1M} and τ_{2M} , respectively. Note that the subscript M in the time constants τ was used to distinguish that the short- and long-time constants are for the discrete Maxwell model. In this model, as $t \rightarrow 0$ of $G(0) = 1$, and at equilibrium, as $t \rightarrow \infty$, the equilibrium normalized elasticity constant, $G(\infty) = G_0/(G_0 + \mu_1/\tau_{1M} + \mu_2/\tau_{2M})$.

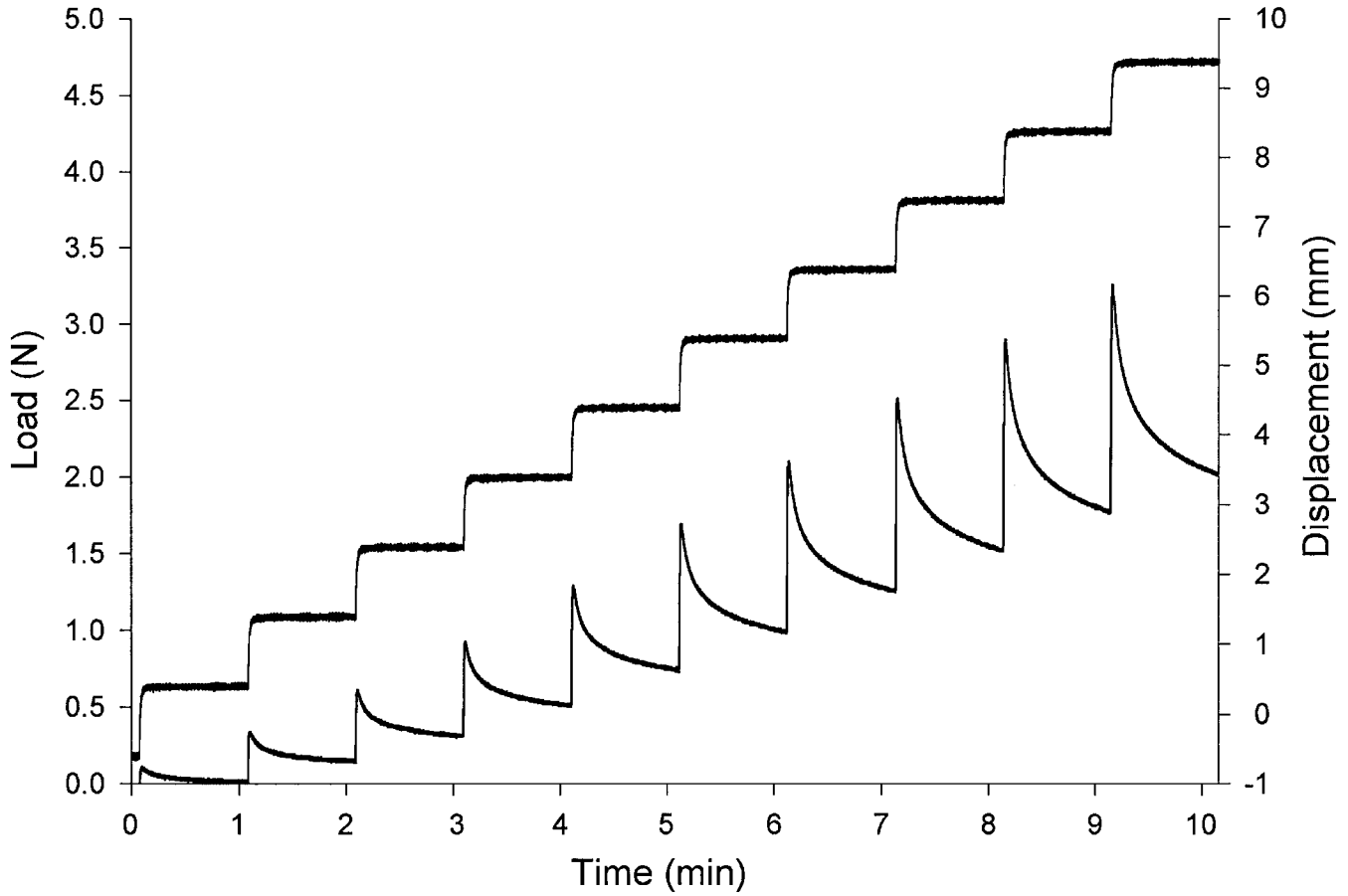


Figure 3. Typical force-time and displacement-time response for subcutaneous tissue.

Reduced Relaxation Function for Continuous Relaxation Spectrum Model

A reduced relaxation function given by Fung [10] was used to describe a continuous spectrum of relaxation times:

$$G(t) = \frac{1 + \int_0^\infty S(\tau)e^{-t/\tau} d\tau}{1 + \int_0^\infty S(\tau) d\tau} \quad (3)$$

where the reduced relaxation function is defined with a limiting value as $t \rightarrow 0$ of $G(0) = 1$, and as $t \rightarrow \infty$, the value of $G(\infty)$ approaches a nonzero constant. The relaxation spectrum $S(\tau)$ described the amplitude of viscous effects as a continuous function of a single variable representing the relaxation time, τ . A relaxation spectrum with constant amplitude of viscous effects over a range of frequencies was originally given by Neubert [20] and is commonly used to describe viscoelastic behaviors of biological materials:

$$S(\tau) = \begin{cases} C/\tau, & \text{for } \tau_{1C} \leq \tau \leq \tau_{2C} \\ 0, & \text{otherwise} \end{cases} \quad (4)$$

This form for relaxation spectrum is particularly suited for describing materials whose stress-strain response is relatively

insensitive to frequency. For this case, as $t \rightarrow \infty$, $G(\infty) = 1/(1 + C * \ln(\tau_{2C}/\tau_{1C}))$. Modifications of this constant amplitude spectrum to describe effects of strain amplitude and rate sensitivity also have been proposed [13, 27].

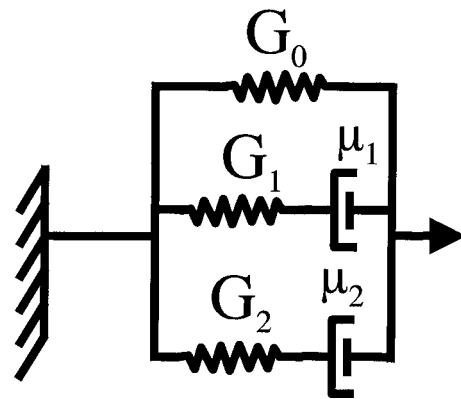


Figure 4. Schematic of 5 parameter Maxwell solid model. Each spring and dashpot represents elastic and viscous components of the material, respectively. The spring constants, G_i , represent the elastic components of the material, whereas the dashpot constants, μ_i , represent viscous components. The viscoelastic time constant may be related to spring and dashpot constants by $\tau_i = \mu_i/G_i$.

Parameter Estimation

Due to the large deformations, strain was calculated as Lagrangian strain [i.e., $1/2*[\lambda^2 - 1]$, where $\lambda = l/l_0$, l_0 is the initial specimen length or the distance between the clamps of the testing machine, and l is the current length), which reduces to infinitesimal strain under small deformations. Total stretch ratio at the end of the experiment was 1.5, while Lagrangian strain was 62.5%. We were unable to precisely describe the sample thickness during testing to determine true stress in a sample. Therefore, engineering stress was calculated from force (obtained at 100 Hz sampling rate) divided by the initial cross-sectional area. Instantaneous (peak) and equilibrium stress-strain responses were calculated. The experimental reduced relaxation function was calculated by dividing the time-dependent stress-relaxation data by the value at $t = 0^+$, just after the step displacement was applied.

The instantaneous tensile modulus, E^e , and equilibrium tensile modulus were determined as the best fit lines to the experimental data describing peak and equilibrium stress values as a function of strain for each test, respectively. The peak stress was evaluated at $t_1 = 10$ ms, where t_1 is the time for acquisition of the first data point after the “step” displacement input. The equilibrium elastic stress data point was taken as the last data point for each test before the next “step” was initiated. Next, the reduced relaxation function was calculated for each step as the transient stress response normalized by the stress response eval-

uated at $t_1 = 10$ ms, i.e., $\sigma(t)/\sigma(t_1)$. Five parameters describing the Maxwell solid model ($G_0, \mu_1, \mu_2, \tau_{1M}, \tau_{2M}$) and three parameters describing the continuous relaxation function (C, τ_{1C}, τ_{2C}) were determined for each step for each specimen using a non-linear least squares regression routine (fminsearch, MATLAB, The Mathworks, Natick, MA, USA). No significant effect of strain was determined for any of the material parameters (using a one way repeated measures ANOVA), and so a single average value for each parameter was determined for each specimen.

Statistical Analysis

The effects of side (left vs. right) and location (dorsal vs. lateral) on the dependent variables ($E^e, G_0, \mu_1, \mu_2, \tau_{1M}, \tau_{2M}, C, \tau_{1C}, \tau_{2C}$) were determined using two-way ANOVA with repeated measures. Fisher’s protected least significant difference (PLSD) post-hoc analyses were used to evaluate the statistical differences among the four groups. Significance was set at $p < .05$ for all statistics.

RESULTS

The mechanical behavior of subcutaneous connective tissue was found to be linear and viscoelastic when subjected to uniaxial tension. The instantaneous (peak) and equilibrium stress-strain response of this tissue were both linear, as demonstrated by values for coefficient of determination, $r^2 = 0.995$ and $r^2 = 0.997$ for peak and equilibrium, respectively (Figure 5). It is

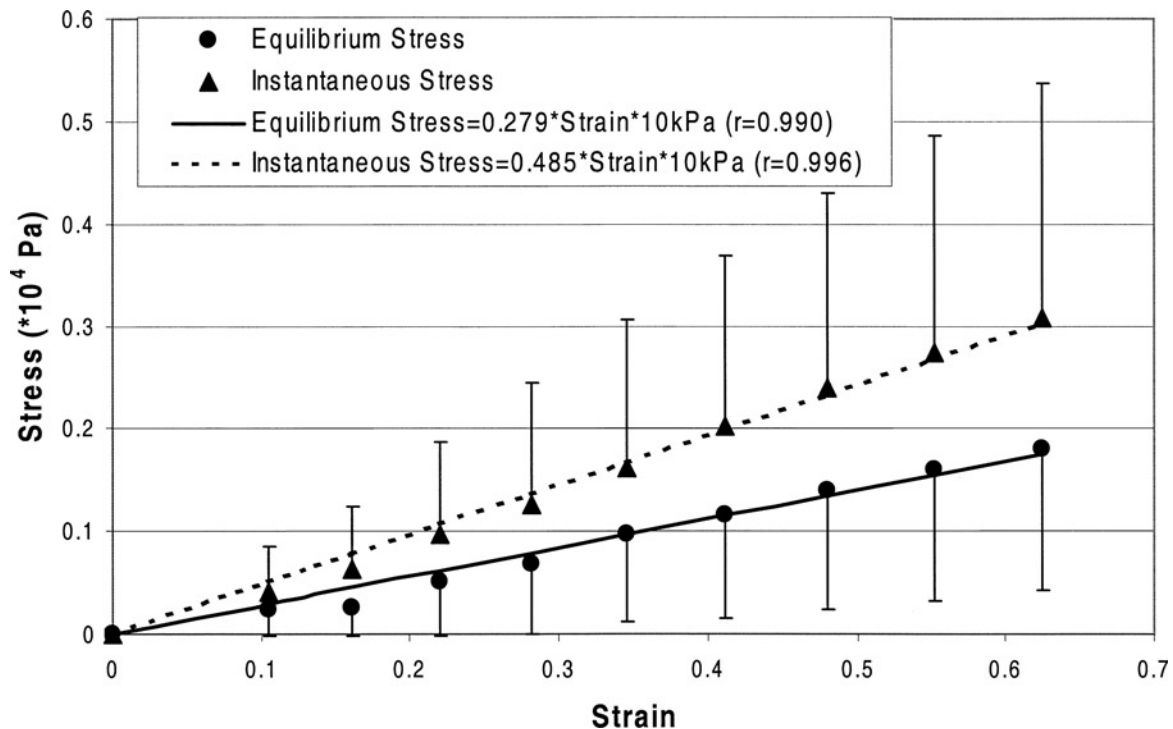


Figure 5. Instantaneous and equilibrium stress-strain curve with linear regressions. Instantaneous and equilibrium data points were taken from the first and last experimental data point for each “step.” The excellent fit of the linear model indicates this tissue exhibits linear stress-strain behaviors. The instantaneous and equilibrium tensile moduli from linear regression of mean data were 4.85 kPa and 2.79 kPa, respectively.

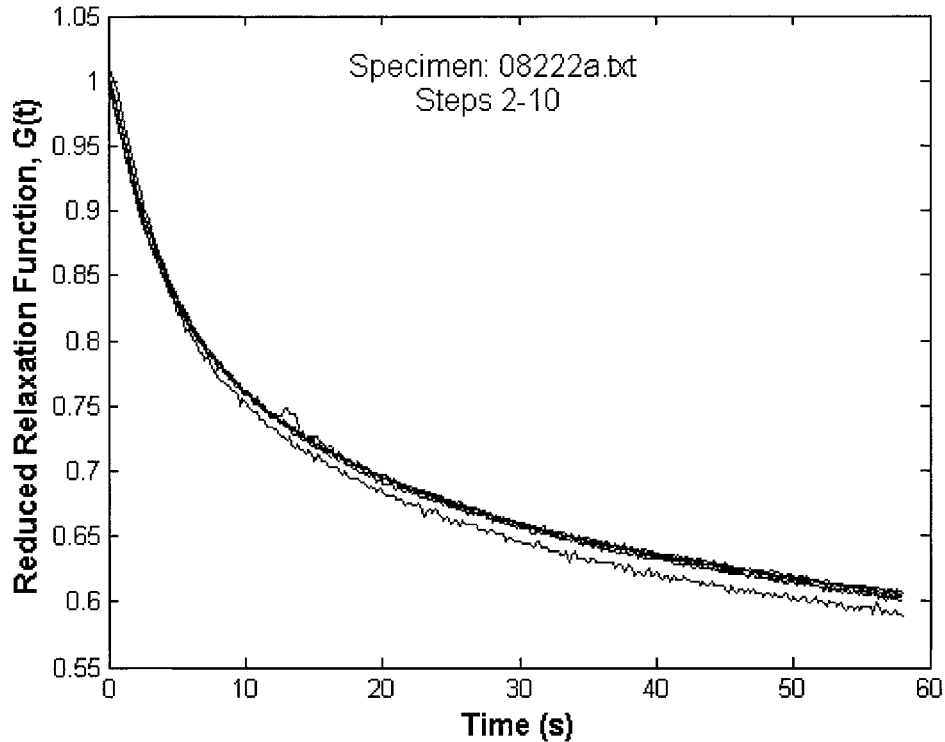


Figure 6. Experimental reduced relaxation function, $G(t)$, for a specimen from the left lateral region. Note that the normalized stress response is similar for all strain values.

notable that the stress-strain curve for each sample and the mean for all samples were linear. The instantaneous and equilibrium tensile moduli from linear regression of mean data were 4.85 kPa and 2.79 kPa, respectively. All specimens remained in the linear stress-strain region up to the 62.5% maximum strain applied and no specimens failed.

The reduced relaxation function for each step superimposed on each specimen was similar for all strain amplitudes (Figure 6). The reduced relaxation function was described well by both the relaxation function with continuous relaxation spectrum, and the 5 parameter Maxwell solid model (Figure 7). Results indicated that parameters describing the relaxation function for each step did not vary as a function of strain for either constitutive model, and therefore for each specimen, average values of the 8 parameters for all steps were calculated.

Average parameter values for all specimens were determined for the 5 parameter Maxwell solid model (Table 1) and the continuous model (Table 2). The Maxwell model and continuous relaxation function predicted that the material relaxed to equilibrium at stress values that were $51 \pm 7\%$ and $51 \pm 8\%$ of the instantaneous elastic stress response, respectively.

The parameters describing the relaxation function were independent of regional location for both models with one exception. For the relaxation function with the continuous relaxation spectrum, no significant effect of location or side was detected for parameters C and τ_{1C} . However, the value of τ_{2C} was larger for the ventral region than for the lateral region, with mean \pm SD

values of 122 ± 26 sec and 99 ± 21 sec, respectively ($p < .05$). We found no significant effects of region for any specimen dimension.

DISCUSSION

The biomechanical behavior of subcutaneous and other soft interstitial connective tissues is largely unknown, yet it is important to understand the effect of mechanical forces on the variety of cells present within this tissue. The objectives of our study were to determine elastic and viscoelastic mechanical properties of ex-vivo rat subcutaneous tissue in uniaxial tension. The first goal was to assess the equilibrium and instantaneous elastic response of this tissue and the second goal was to define the tissue's viscoelastic behaviors. The tensile behavior of subcutaneous connective tissue was linearly elastic and its viscoelastic parameters were relatively insensitive to strain rate.

The equilibrium and instantaneous elastic response of subcutaneous tissue was highly linear up to 50% strain. This highly linear response from 5% to 50% strain contrasts with the behavior of skin and many other connective tissues that often have distinct nonlinear regions in uniaxial tension where the tissue stiffens (i.e., the slope of the stress-strain curve increases) as the strain increases and more fibers are recruited to carry tensile loads [1, 5, 7, 15, 16, 22, 23, 25]. The linear response of subcutaneous connective tissue suggests that the structural components of the tissue are already recruited and bearing load under our loading conditions.

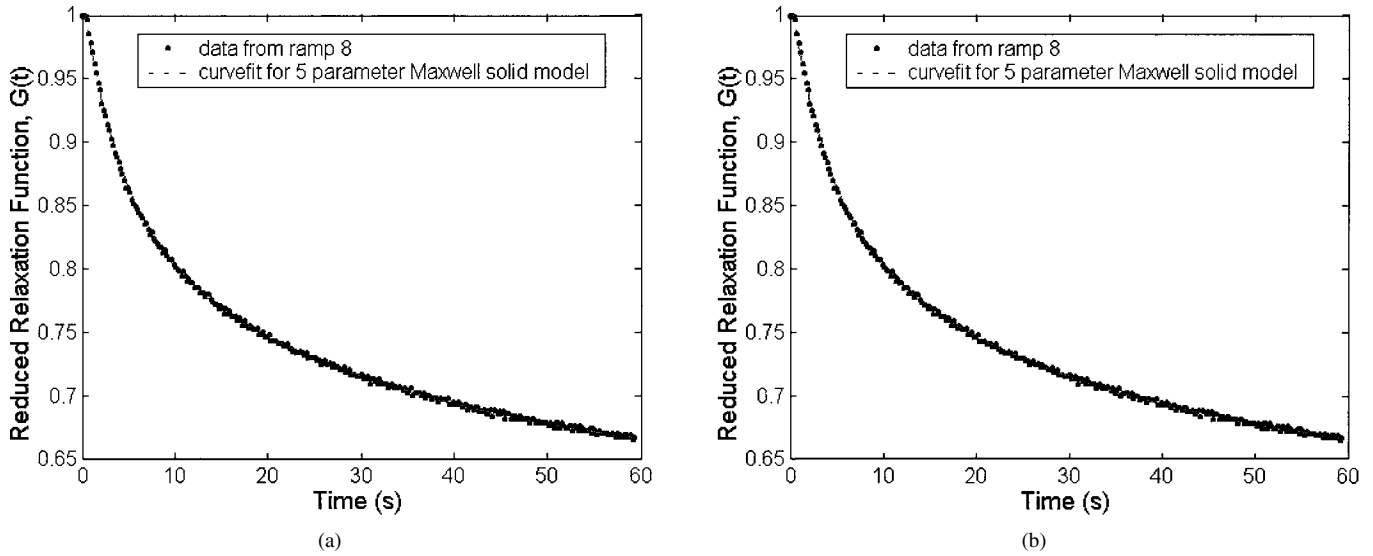


Figure 7. Typical plot of normalized stress and curvefit for (a) 5 parameter Maxwell solid model and (b) continuous relaxation function. Parameters for the curvefit of 5 parameter Maxwell model for this specimen are $G(\infty) = 0.6362$; $\tau_{1M} = 4.222$ sec; $\tau_{2M} = 31.24$ sec; $\mu_1 = 0.7317$ (N · s/m); $\mu_2 = 6.4448$ (N · s/m); $R = 0.999$. Parameters for the curvefit of the continuous relaxation function of this specimen are $C = 0.15967$; $\tau_{1C} = 2.2691$ s; $\tau_{2C} = 110.5756$ s; $R = 0.998$. The goodness of fit of the continuous model indicates the material parameters were relatively insensitive to strain-rate.

When comparing other tissues, we observed that tensile failure strain is relatively low when highly structured tissues are tested in the direction of the predominant fiber orientation; e.g., intervertebral disc annulus (<15%) [26], ligaments (<20%) [30], cartilage (50%) [23], and acetabular labrum (<30%) [7]. When tested perpendicular to the predominant fiber direction however, these tissues exhibit tensile failure strains that are much larger and typically above 50%: e.g., intervertebral disc annulus (>70%) [9], cartilage (>100%) [23]. When tested transverse to the predominant fiber direction, it is largely the noncollagenous matrix of the tissue and not the fibers that define the failure strain.

The failure strain of gastrointestinal tissue, on the other hand, did not exhibit significant effects of tensile testing direction fiber with failure strains >100% [4]. Investigation of yield and failure behaviors of subcutaneous connective tissue will be the subject of future investigation. Yet failure strain is clearly greater than 50% which suggests that it is likely to be the “ground substance” and not collagen fibers that are defining the material behavior of subcutaneous connective tissue. Our preliminary testing demonstrated that beyond the linear region the subcutaneous connective

tissue began to yield and soften with strain (i.e., the slope of the stress-strain curve decreased with strain amplitude) characteristic of a rubber-like response. Due to the relatively high-yield strain, it is likely that the tissue stays in the linear region under physiological loading in vivo, and use of quasilinear or nonlinear viscoelastic models is unnecessary. However, it is possible that therapies involving connective tissue stretch (such as physiotherapy, massage, or acupuncture) may subject this tissue to supraphysiological amounts of strain.

The tensile modulus of subcutaneous connective tissue reported in this study is similar to that for skin at low strains (<10%) [5] but orders of magnitude lower than many other solid tissues in the body (Table 3). Eshel and Lanir [5] proposed that elastin and proteoglycans dominated the low and intermediate strain responses of skin while collagen dominated the high strain response. This conceptual model suggests that elastin and proteoglycans in subcutaneous tissue may dominate its mechanical behavior. In contrast, the tensile modulus of skin under high strains is approximately 240 kPa; most orthopedic tissues have tensile moduli at least 1 MPa, while tissues of the eye (choroidal complex, sclera, lens) range from 600–23,000 kPa. The nucleus

TABLE 1

Mean ± SD of all specimens ($n = 20$) values for 5 parameter Maxwell solid relaxation function with discrete relaxation spectrum.

$G(\infty)$	μ_1 (N · s/m)	μ_2 (N · s/m)	τ_{1M} (s)	τ_{2M} (s)
0.51 ± 0.07	0.95 ± 0.24	8.49 ± 2.42	3.83 ± 0.15	30.15 ± 3.16

The parameter G_0 defines the equilibrium elastic response. The parameters μ_i defined coefficients of viscosity which had associated time constants, τ_{iM} .

TABLE 2

Mean ± SD values of all specimens ($n = 20$) for parameters defining the relaxation function with continuous relaxation spectrum.

$G(\infty)$	C	τ_{1C} (s)	τ_{2C} (s)
0.51 ± 0.01	0.25 ± 0.03	1.86 ± 0.30	110.40 ± 11.80

The parameters C , τ_{1C} , and τ_{2C} defined the magnitude and time limits of the relaxation spectrum. No effect of location (ventral or lateral) or side (left or right) were detected for C or τ_1 .

TABLE 3

Equilibrium tensile elastic modulus for several connective tissues taken from the literature.

Tissue	Equilibrium tensile modulus (kPa)	Reference
Synovial fluid (dynamic shear modulus)	0.02	[24]
Chondrocyte (instantaneous elastic modulus)	0.52	[29]
Pericellular matrix of the cell	1.54	[11]
<i>Subcutaneous tissue</i>	2.75	<i>This study</i>
Rat dorsal skin (low strains)	4.8	[5]
Rat skin (high strains)	240	[5, 22]
Nucleus pulposus (instantaneous shear modulus)	11	[14]
Annulus fibrosus	470 (perpendicular to fibers)	[9]
	88,000 (parallel to fibers)	[26]
Choroidal complex of eye	600	[8]
Gastrointestinal tract	1600	[4]
Sclera	2900	[8]
Articular cartilage	1,000–43,000	[19]
Lens capsule	23,000	[17]
Knee meniscus	40,000–60,000	[19]
Acetabular labrum	74,650	[7]
Medial collateral ligament	780,000	[31]

For more highly “fluid-like” tissues, the tensile moduli are unavailable and shear moduli are given.

pulposus of the spinal disc had an elastic modulus of the same order of magnitude as subcutaneous tissue, yet the nucleus is often considered a fluid because of its very low equilibrium stress values [14]. The low modulus of subcutaneous connective tissue suggests that this tissue does not bear high loads but may function to transmit mechanical signals to and from the cells. It is interesting to note the modulus of subcutaneous connective tissue is similar to that of the pericellular matrix of articular chondrocytes [11, 29].

The viscoelastic relaxation spectrum parameters for subcutaneous connective tissue had an initial relaxation time (τ_{1C}) that was longer and the time to reach equilibrium (as measured by τ_{2C}) was relatively shorter than several other tissues in the literature. For example, ligament tissue tested in tension, had values for C , τ_{1C} , and τ_{2C} of 0.146, 0.1 sec and 80,800 sec, respectively [15, 30, 31]. For the intervertebral disc nucleus pulposus in shear, the values for C , τ_{1C} , and τ_{2C} are 1.6, 0.048 sec and 600 sec, respectively. It is interesting to note that not only does subcutaneous connective tissue relax more quickly than other tissues, but

also its equilibrium-to-peak-stress ratio is rather high, with values of equilibrium normalized elasticity constant $G(\infty) = 0.51$, 0.33, and 0.03 for subcutaneous connective tissue, ligament, and nucleus pulposus, respectively [13, 31]. The short-time relaxation time constant of subcutaneous connective tissue was close to that for skin ($\tau = 6.3$ sec) [22] and approaches that of articular chondrocytes ($\tau = 0.92$ sec) [11, 29].

Both forms for relaxation function fit the experimental data extremely well. We reported values for both the 5 parameter Maxwell model and the continuous relaxation function to provide a choice to the user. The continuous relaxation spectrum only requires 3 parameters, yet closed-form solutions for Equation (1) are impossible because the exponential integral requires numerical approximations. The 5 parameter Maxwell solid model requires more material parameters yet analytical solutions are relatively straightforward for the series of exponentials. Both models demonstrate relative insensitivity of the tissue to strain rate because our relaxation spectrum (defined with the 5 parameter model) had a nearly constant amplitude ($\mu_1/\tau_{1M} \approx \mu_2/\tau_{2M}$), and we were able to accurately describe the material behavior with the continuous relaxation function (which requires strain rate insensitivity because of the constant amplitude continuous relaxation spectrum).

A potential limitation of this study is that there may be a small toe region in our tissue that was not detected because of our 5% strain increments. However, it is clear that any nonlinearities will occur at very small strains relative to the failure strain of the tissue. Future studies are necessary to investigate failure mechanisms, to more precisely define structure-function relationships, and to isolate the contribution of cells to the mechanical properties of subcutaneous connective tissue. Our volume determinations and hence cross-sectional area did not account for potential volume changes resulting from equilibration in Hapes buffer which caused the tissue to swell, thereby overestimating the cross-sectional area and underestimating the stress response. This was done to ensure stable dimensions during testing and to facilitate comparison with other tissues (since in vitro tissue mechanical properties are typically obtained when the tissue is equilibrated in solution). There was no evidence of mechanical damage under the range of strains tested (as tests to larger strains demonstrated a loss of linearity of stress-strain response as failure initiated) and the relatively short-time constants for this tissue suggested that changes in volume due to testing or viscoelastic effects were minimal.

Theoretical models demonstrate that the tissue behavior is insensitive to strain rate. Further experiments would be required to test this assumption more robustly or over larger ranges of frequencies. The value we report for equilibrium stress (and modulus) may slightly overestimate the actual values as each incremental stress relaxation experiment had a 60-sec duration and equilibrium was not always achieved. Theoretically, however, we calculate an equilibrium modulus as 51% of the instantaneous modulus, or $4.77 \text{ kPa} \cdot 0.51 = 2.43 \text{ kPa}$, which is slightly lower than the experimentally determined value of 2.75 kPa.

Although the aim of this study was not to test for differences in viscoelastic behavior between body regions (in this case ventral versus lateral abdominal wall), we did find that one of the parameters (τ_{2C}) was larger for the ventral region than for the lateral region, indicating that tissue in the ventral region took longer for the stress to relax to equilibrium. This may have been due to a difference in the ratio of fat to collagen that, based on our histological observation, tends to be greater in the lateral compared with the ventral region. Alternatively, there may be differences in other matrix components (e.g., elastic fibers, glycosaminoglycans) between these regions. We did not find regional differences for the other parameters, though this may be due to sample size. Power calculations indicated that our statistical power was 0.80 (using $\alpha = 0.05$) to detect a mean difference of 22–35% between regions for all outcome measures except for parameter C for which our power was 0.80 to detect a 100% difference.

CONCLUSION

In sum, rat subcutaneous tissue ex-vivo was linearly elastic with time-dependent viscoelastic behaviors that were relatively insensitive to strain-rate. The experimental behaviors were well described using a 5 parameter Maxwell solid model and using a continuous relaxation function with constant amplitude relaxation spectrum. Subcutaneous tissue had a very low tensile modulus that was closer to the properties of skin under low strains, the nucleus pulposus of the intervertebral disc, or pericellular matrix of chondrocytes than that of many other connective tissues. The ratio of peak (instantaneous) to equilibrium tensile modulus (a measure of the relative amount of viscoelasticity) also is relatively high and closer to the value for cells than many other connective tissues. Our results provide baseline information for the stress-strain behaviors of subcutaneous connective tissue and underscore the differences in mechanical behaviors between loose and high-load bearing connective tissues.

This “whole tissue” mechanical behavior may be directly relevant to mechanical signal transduction processes occurring at the cellular level and to the impact of mechanical forces on the abundant fibroblasts, immune, vascular, and neural cells present within these tissues. The elastic and viscoelastic behavior of loose connective tissues thus may be an important factor determining the many potential cellular effects of therapies utilizing mechanical stretch, as well as normal movement and exercise.

ACKNOWLEDGMENT

Support for this work comes from National Institutes of Health, National Center for Complementary and Alternative Medicine grant AT001121, and National Institute of Arthritis, Musculoskeletal and Skin Diseases grant AR02078. We thank Gary J. Badger, MS, for assistance with statistical analyses.

REFERENCES

- [1] Acaroglu, E.R., Iatridis, J.C., Setton, L.A., et al. (1995). Degeneration and aging affect the tensile behavior of human lumbar annulus fibrosus. *Spine* 20:2690–2701.
- [2] Banes, A.J., Tszuzaki, M., Yamamoto, J., et al. (1995). Mechanoreception at the cellular level: The detection, interpretation, and diversity of responses to mechanical signals. *Biochem. Cell Biol.* 73:349–365.
- [3] Darby, R. (1976). *Viscoelastic Fluids*. New York: Marcel Dekker.
- [4] Egorov, V., Schastlivtsev, I., Prut, E., et al. (2002). Mechanical properties of the human gastrointestinal tract. *J. Biomech.* 35:1417.
- [5] Eshel, H., and Lanir, Y. (2001). Effects of strain level and proteoglycan depletion on preconditioning and viscoelastic responses of rat dorsal skin. *Ann. Biomed. Eng.* 29:164–172.
- [6] Fawcett, D.W. (1994). *Connective tissue. A Textbook of Histology*. New York: Chapman and Hall.
- [7] Ferguson, S.J., Bryant, J.T., and Ito, K. (2001). The material properties of the bovine acetabular labrum. *J. Orthop. Res.* 19:887–896.
- [8] Friberg, T.R., and Lace, J.W. (1988). A comparison of the elastic properties of human choroid and sclera. *Exp. Eye Res.* 47:429–436.
- [9] Fujita, Y., Duncan, N.A., and Lotz, J.C. (1997). Radial tensile properties of the lumbar annulus fibrosus are site and degeneration dependent. *J. Orthop. Res.* 15:814–819.
- [10] Fung, Y.C. (1993). *Biomechanics: Mechanical Properties of Living Tissues*. New York: Springer-Verlag.
- [11] Guilak, F., Jones, W.R., Ting-Beall, H.P., et al. (1999). The deformation behavior and mechanical properties of chondrocytes in articular cartilage. *Osteoarth. Cart.* 7:59–70.
- [12] Hardy, M., and Woodall, W. (1998). Therapeutic effects of heat, cold, and stretch on connective tissue. *J. Hand Ther.* 11:148–156.
- [13] Iatridis, J.C., Setton, L.A., Weidenbaum, M., et al. (1997). The viscoelastic behavior of the non-degenerate human lumbar nucleus pulposus in shear. *J. Biomech.* 30:1005–1013.
- [14] Iatridis J.C., Weidenbaum, M., Setton, L.A., et al. (1996). Is the nucleus pulposus a solid or a fluid? Mechanical behaviors of the nucleus pulposus of the human intervertebral disc. *Spine* 21:1174–1184.
- [15] Johnson, G.A., Tramaglino, D.M., Levine, R.E., et al. (1994). Tensile and viscoelastic properties of human patellar tendon. *J. Orthop. Res.* 12:796–803.
- [16] Kempson, G.E. (1991). Age-related changes in the tensile properties of human articular cartilage: A comparative study between the femoral head of the hip joint and the talus of the ankle joint. *Biochim. Biophys. Acta* 1075:223–230.
- [17] Krag, S., and Andreassen, T.T. (1996). Biomechanical measurements of the porcine lens capsule. *Exp. Eye Res.* 62:253–260.
- [18] Langevin, H.M., Churchill, D.L., Wu, J., et al. (2002). Evidence of connective tissue involvement in acupuncture. *FASEB J.* 16:872–874.
- [19] Mow, V.C., and Ratcliffe, A. (1997). Structure and function of articular cartilage and meniscus. In *Basic Orthopaedic Biomechanics*, V.C. Mow and W.C. Hayes (eds.), pp. 113–177. Philadelphia: Lippincott-Raven.
- [20] Neubert, H.K.P. (1963). A simple model representing internal damping in solid materials. *Aeronaut Q.* 14:187–197.
- [21] Oschman, J.L. (1993). *Readings on the Scientific Basis of Body Work*. Dover, NH: Nature’s Own Research Association.
- [22] Oxlund, H., Manschot, J., and Viidik, A. (1988). The role of elastin in the mechanical properties of skin. *J. Biomech.* 21:213–218.
- [23] Roth, V., and Mow, V.C. (1980). The intrinsic tensile behavior of the matrix of bovine articular cartilage and its variation with age. *J. Bone Joint Surg. Am.* 62:1102–1117.
- [24] Safari, M., Bjelle, A., Gudmundsson, M., et al. (1990). Clinical assessment of rheumatic diseases using viscoelastic parameters for synovial fluid. *Biorheology* 27:659–674.
- [25] Simon, B.R., Coats, R.S., and Woo, S.L. (1984). Relaxation and creep quasilinear viscoelastic models for normal articular cartilage. *J. Biomech. Eng.* 106:159–164.
- [26] Skaggs, D.L., Weidenbaum, M., Iatridis, J.C., et al. (1994). Regional variation in tensile properties and biochemical composition of the human lumbar annulus fibrosus. *Spine* 19:1310–1319.

- [27] Spirt, A.A., Mak, A.F., and Wassell, R.P. (1989). Nonlinear viscoelastic properties of articular cartilage in shear. *J. Orthop. Res.* 7:43–49.
- [28] Threlkeld, A.J. (1992). The effects of manual therapy on connective tissue. *Phys. Ther.* 72:893–902.
- [29] Trickey, T.R., Lee, M., and Guilak, T. (2000). Viscoelastic properties of chondrocytes from normal and osteoarthritic human cartilage. *J. Orthop. Res.* 18:891–898.
- [30] Woo, S.L., Gomez, M.A., Inoue, M., et al. (1987). New experimental procedures to evaluate the biomechanical properties of healing canine medial collateral ligaments. *J. Orthop. Res.* 4:425–432.
- [31] Woo, S.L.Y., Livesay, G.A., Runco, T.J., et al. (1997). Structure and function of tendons and ligaments. In *Basic Orthopaedic Biomechanics*, V.C. Mow and W.C. Hayes (eds.), pp. 209–251. Philadelphia: Lippincott-Raven.